ELSEVIER

Signal Processing: *Image Communication* 16 (2001) 541–551

SIGNAL PROCESSING: IMAGE COMMUNICATION

www.elsevier.nl/locate/image

Approximation of the Karhunen–Loève transformation and its application to colour images

Rémi Kouassi, Pierre Gouton*, Michel Paindavoine

Laboratoire d'Electronique, d'Informatique et d'Image, Aile des Sciences de l'Ingénieur – BP 47870, 21078 Dijon Cedex, France

Abstract

Analysis of colour images in the Red, Green and Blue acquisition space and in the intensity and chrominance spaces shows that colour components are closely correlated (Carron, Ph.D. Thesis, Univ. Savoie, France, 1995; Ocadis, Ph.D. Thesis, Univ. Grenoble, France, 1985). These have to be decorrelated so that each component of the colour image can be studied separately. The Karhunen–Loève transformation provides optimal decorrelation of these colour data. However, this transformation is related to the colour distribution in the image, i.e. to the statistical properties of the colour image and is therefore dependent on the image under analysis. In order to enjoy the advantages of direct, independent and rapid transformation and the advantages of the Karhunen–Loève properties, this paper presents the study of the approximation of the Karhunen–Loève transformation. The approximation is arrived at through exploitation of the properties of Toeplitz matrices. The search for eigenvectors of a Toeplitz matrix shows that complex or real orthogonal mappings such as the discrete Fourier transform and its decompositions approximate the Karhunen–Loève transformation in the case of first-order Markov processes.

Keywords: Colour analysis; Toeplitz matrix; Toeplitz matrix eigenvalues and vectors; First-order stationary process; Karhunen–Loève transformation; Discrete sine and discrete cosine transformations

1. Introduction

In order to study a colour image, it is first necessary to define the base in which the colour image is represented. Several investigations have looked at the representation systems to find the base that best renders the colour [6]. The best-known colour image representation spaces are the RGB system (Red, Green, Blue) of the Commission Internationale pour l'Éclairage (CIE) and the $R_N G_N B_N$ system of the National Television Standard Chromacity (NTSC) for colour image acquisition [7]; most colour cameras operate with these two systems. There are also intensity and chrominance spaces for separating luminance and colour. But the hue and saturation components defining the colour plane are closely related [1]. By using the Karhunen–Loève development to represent colour images, the different colour components can be treated separately [3].

* Corresponding author.
E-mail address: pgouton@u-bourgogne.fr (P. Gouton).

0923-5965/01/$ - see front matter
PII: S0923-5965(00)00035-7

Indeed, the Karhunen–Loève development – or principle data component representation – is a dependable statistical means of characterising the data set main axes [5]. The main axes will therefore define the colour image representation axes. However, the Karhunen–Loève transformation cannot be applied just once for the entire set of images to be processed. The transformation matrix must be re-calculated for each colour image. Accordingly, to take advantage of the Karhunen–Loève–Loève representation and a fixed transformation, we investigate here the approximation of the Karhunen–Loève space by linear orthogonal transformations. Several papers show that orthogonal transformations are asymptotically equivalent to the Karhunen–Loève transformation when there is a large number of principle vectors [2,4,9,10]. In this paper we show that Karhunen–Loève space can be approximated by linear orthogonal space with a limited number of three base vectors.

A colour image is stationary or homogeneous if its correlation matrix is similar to that of a first-order Markov process. In this case, the distribution of the information on the three axes of the acquisition space (RGB) is uniformly spread. Our approach is based on the properties of stationary systems and of Toeplitz matrices. The objective being to obtain a Karhunen–Loève-type transformation that is independent of the image to be processed; we develop a method to show that the colour image covariance matrix can be diagonalised by DFT, DOFT, DREFT, DROFT, DCT and DEST orthogonal transformations [8].

Section 2 of the paper concentrates on the definition of the Karhunen–Loève transformation and the approximation from a colour covariance matrix to a Toeplitz matrix. Section 3 is an analysis of the properties of Toeplitz matrices to estimate their eigenvalues and eigenvectors. Finally, in Section 4, we apply the results of the approximation of Karhunen–Loève space to colour images that are representative of natural scenes.

2. Karhunen–Loève transformation in the case of colour images

2.1. Determining the colour image covariance matrix and the Karhunen–Loève transformation matrix

2.1.1. Calculating the covariance matrix

The covariance matrix of a colour is defined by the following expression:

$$C_T = E\{(T - m_T)(T - m_T)'\} \tag{1}$$

where m_T is the colour image mean vector, E is the mathematical expectation and T the colour image vector,

$$m_T = E\{T\}. \tag{2}$$

Matrix C_T can be written as

$$C_T = \frac{1}{N}\sum_{i=1}^{N} (T_i - m_T)(T_i - m_T)', \tag{3}$$

N is the total number of pixels in the image.

Developing Eq. (3) gives the following covariance matrix for the colour image:

$$C_T = C_{RGB} = \begin{vmatrix} c_{RR} & c_{RG} & c_{RB} \\ c_{RG} & c_{GG} & c_{GB} \\ c_{RB} & c_{GB} & c_{BB} \end{vmatrix} = \begin{vmatrix} c_{11} & c_{12} & c_{13} \\ c_{21} & c_{22} & c_{23} \\ c_{31} & c_{32} & c_{33} \end{vmatrix}. \tag{4}$$

R, G and B are the Red, Green and Blue components of the colour image, respectively. The order of the components is irrelevant in calculating the covariance matrix; the order RGB, RBG, GRB, GBR, BGR or BRG can be defined without altering the structure or eigenvalues and eigenvectors of the colour image

covariance matrix. The image correlation matrix is then obtained directly from its covariance matrix:

$$\varphi_T = \left[\frac{c_{ij}}{\sqrt{c_{ii}c_{jj}}}\right] = \begin{pmatrix} \frac{c_{11}}{\sqrt{c_{11}c_{11}}} & \frac{c_{12}}{\sqrt{c_{11}c_{22}}} & \frac{c_{13}}{\sqrt{c_{11}c_{33}}} \\ \frac{c_{21}}{\sqrt{c_{22}c_{11}}} & \frac{c_{22}}{\sqrt{c_{22}c_{22}}} & \frac{c_{23}}{\sqrt{c_{22}c_{33}}} \\ \frac{c_{31}}{\sqrt{c_{33}c_{11}}} & \frac{c_{32}}{\sqrt{c_{33}c_{22}}} & \frac{c_{33}}{\sqrt{c_{33}c_{33}}} \end{pmatrix}. \tag{5}$$

The covariance matrix is symmetrical. If we further assume that it is a Toeplitz matrix (i.e. that coefficients c_{11}, c_{22} and c_{33} are equal and that coefficients c_{12} and c_{23} are equal) then the colour image correlation matrix is quite similar to that of a first-order Markov process. In this specific instance, the image is homogeneous or stationary. The correlation matrix of a first-order Markov process is expressed below [2]:

$$\begin{pmatrix} 1 & \varphi & \varphi^2 \\ \varphi & 1 & \varphi \\ \varphi^2 & \varphi & 1 \end{pmatrix}, \tag{6}$$

φ is the correlation coefficient between zero and one.

For what follows, we concentrate on the first-order stationary processes.

2.2. Calculating the Karhunen–Loève transformation matrix

The Karhunen–Loève transformation equation is defined by

$$U = A(T - m_T). \tag{7}$$

In this expression, U is the transformed image vector, T is the original colour image vector in the RGB colour representation space and A the transformation matrix. It is the matrix of eigenvalues of the colour image covariance matrix. The Karhunen–Loève transformation is therefore defined by the search for the covariance matrix eigenvalues. These eigenvalues are the basis of the Karhunen–Loève representation.

3. Search for the eigenvectors of a Toeplitz matrix

3.1. Search for the eigenvalues of a Toeplitz matrix

Consider the following Toeplitz matrix:

$$C_3 = \begin{vmatrix} c_0 & c_1 & c_2 \\ c_1 & c_0 & c_1 \\ c_2 & c_1 & c_0 \end{vmatrix}. \tag{8}$$

The circular decomposition of a matrix is obtained by the sum of the circular matrices. We decompose matrix C_3 defined above from the circular A_3 and pseudo-circular B_3 matrices. For this we consider that matrix D_3 obtained by inverting the elements of each line of matrix C_3 without altering the elements on the

diagonal:

$$D_3 = \begin{vmatrix} c_0 & c_2 & c_1 \\ c_2 & c_0 & c_2 \\ c_1 & c_2 & c_0 \end{vmatrix}, \tag{9}$$

D_3 is also a symmetrical Toeplitz matrix.

The circular A_3 and pseudo-circular B_3 matrices are defined as follows:

$$A_3 = \frac{1}{2}(C_3 + D_3) = \begin{vmatrix} c_0 & \frac{c_1 + c_2}{2} & \frac{c_1 + c_2}{2} \\ \frac{c_1 + c_2}{2} & c_0 & \frac{c_1 + c_2}{2} \\ \frac{c_1 + c_2}{2} & \frac{c_1 + c_2}{2} & c_0 \end{vmatrix}, \tag{10}$$

$$B_3 = \frac{1}{2}(C_3 - D_3) = \begin{vmatrix} 0 & \frac{c_1 - c_2}{2} & \frac{c_2 - c_1}{2} \\ \frac{c_1 - c_2}{2} & 0 & \frac{c_1 - c_2}{2} \\ \frac{c_2 - c_1}{2} & \frac{c_1 - c_2}{2} & 0 \end{vmatrix}. \tag{11}$$

Circular decomposition of matrix C_3 is then obtained from the relation

$$C_3 = A_3 + B_3. \tag{12}$$

Matrices A_3 and B_3 are also Toeplitz symmetrical matrices.

3.2. Diagonalising a Toeplitz matrix

To calculate the eigenvalues and eigenvectors for diagonalising matrix C_3, we seek instead to diagonalise matrices A_3 and B_3. We then consider the permutation matrices P_3 and Q_3 defined below:

$$P_3 = \begin{vmatrix} 0 & 1 & 0 \\ 0 & 0 & 1 \\ 1 & 0 & 0 \end{vmatrix}, \qquad Q_3 = \begin{vmatrix} 0 & 1 & 0 \\ 0 & 0 & 1 \\ -1 & 0 & 0 \end{vmatrix}. \tag{13}$$

The circular matrix A_3 and the pseudo-circular matrix B_3 can then be expressed as polynomial functions of permutation matrices P_3 and Q_3. This gives the following relations:

$$A_3 = \sum_{k=0}^{2} a_k P_3^k \quad \text{and} \quad B_3 = \sum_{k=0}^{2} b_k Q_3^k. \tag{14}$$

By writing matrices A_3 and B_3 in polynomial form we can define their eigenvalues from those of matrices P_3 and Q_3. The eigenvalues are also related by the same polynomial relations, i.e. if we denote as λ_a, λ_p, μ_b and μ_q, respectively, the eigenvalues of matrices A_3, P_3, B_3 and Q_3, we can then write

$$\lambda_a = \sum_{k=0}^{2} a_k \lambda_p^k \quad \text{and} \quad \mu_b = \sum_{k=0}^{2} b_k \mu_q^k. \tag{15}$$

It is obvious that as matrices P_3 and Q_3 are very simple (composed of ones and zeroes), their eigenvalues and eigenvectors can be calculated easily. This gives the following noteworthy expressions:

$$P_3: \quad \lambda_1 = 1, \quad \lambda_2 = \exp\left(\frac{2\pi}{3}\mathrm{j}\right), \quad \lambda_3 = \exp\left(-\frac{2\pi}{3}\mathrm{j}\right), \tag{16}$$

$$Q_3: \quad \mu_1 = -1, \quad \mu_2 = \exp\left(\frac{\pi}{3}\mathrm{j}\right), \quad \mu_3 = \exp\left(-\frac{\pi}{3}\mathrm{j}\right). \tag{17}$$

By using formula (14) we determine the eigenvalues of matrices A_3 and B_3.

$$A_3: \quad \lambda_i^a = \sum_{k=0}^{2} a_k \lambda_i^k = \sum_{k=0}^{2} a_k \exp\left(\pm\frac{2\pi(i-1)k}{3}\mathrm{j}\right), \quad i = 1,2,3, \tag{18}$$

$$B_3: \quad \mu_i^b = \sum_{k=0}^{2} b_k \mu_i^k = \sum_{k=0}^{2} b_k \exp\left(\pm\frac{\pi(2i-1)k}{3}\mathrm{j}\right), \quad i = 1,2,3. \tag{19}$$

The eigenvectors corresponding to the eigenvalues of matrices P_3 and A_3 are formulated as follows:

$$U_m(k) = \frac{1}{\sqrt{3}} \exp\left(\pm\frac{\mathrm{j}2\pi(m-1)(k-1)}{3}\right), \quad k,m = 1,2,3. \tag{20}$$

This formula is nothing other than the discrete Fourier transform (DFT). The circular matrix A_3 can therefore be diagonalised by the discrete Fourier transform matrix.

By developing this expression, the three eigenvectors of matrix A_3 can be given as

$$U_1 = \begin{vmatrix} u_{11} \\ u_{12} \\ u_{13} \end{vmatrix} = \frac{1}{\sqrt{3}} \begin{vmatrix} 1 \\ 1 \\ 1 \end{vmatrix}, \qquad U_2 = \begin{vmatrix} u_{21} \\ u_{22} \\ u_{23} \end{vmatrix} = \frac{1}{\sqrt{3}} \begin{vmatrix} 1 \\ -\frac{1}{2} + \mathrm{j}\frac{\sqrt{3}}{2} \\ -\frac{1}{2} - \mathrm{j}\frac{\sqrt{3}}{2} \end{vmatrix}, \qquad U_3 = \begin{vmatrix} u_{31} \\ u_{32} \\ u_{33} \end{vmatrix} = \frac{1}{\sqrt{3}} \begin{vmatrix} 1 \\ -\frac{1}{2} - \mathrm{j}\frac{\sqrt{3}}{2} \\ -\frac{1}{2} + \mathrm{j}\frac{\sqrt{3}}{2} \end{vmatrix}. \tag{21}$$

Likewise, the eigenvectors of matrices Q_3 and B_3 are calculated, giving

$$V_m(k) = \frac{1}{\sqrt{3}} \exp\left(\pm\frac{\mathrm{j}\pi(2m-1)(k-1)}{3}\right), \quad k,m = 1,2,3. \tag{22}$$

The expression of the eigenvectors is that of the discrete odd Fourier transform. Thus, the development of the expression below means the eigenvectors of matrix B_3 can be written out completely:

$$V_1 = \begin{vmatrix} v_{11} \\ v_{12} \\ v_{13} \end{vmatrix} = \frac{1}{\sqrt{3}} \begin{vmatrix} 1 \\ -1 \\ 1 \end{vmatrix}, \qquad V_2 = \begin{vmatrix} v_{21} \\ v_{22} \\ v_{23} \end{vmatrix} = \frac{1}{\sqrt{3}} \begin{vmatrix} 1 \\ \frac{1}{2} - \mathrm{j}\frac{\sqrt{3}}{2} \\ -\frac{1}{2} - \mathrm{j}\frac{\sqrt{3}}{2} \end{vmatrix}, \qquad V_3 = \begin{vmatrix} v_{31} \\ v_{32} \\ v_{33} \end{vmatrix} = \frac{1}{\sqrt{3}} \begin{vmatrix} 1 \\ \frac{1}{2} + \mathrm{j}\frac{\sqrt{3}}{2} \\ -\frac{1}{2} + \mathrm{j}\frac{\sqrt{3}}{2} \end{vmatrix}. \tag{23}$$

The eigenvectors of matrices A_3 and B_3 having been determined, it is possible to calculate those of matrix C_3 by using the relation linking a matrix to its eigenvalues and eigenvectors. The equations below are obtained:

$$A_3 U = \lambda U, \tag{24}$$

$$B_3 V = \mu V. \tag{25}$$

By denoting as $(\tilde{U})$ a combination of vectors U and V, we obtain the equations given below:

$$A_3 \tilde{U} = \lambda \tilde{U}, \tag{26}$$

$$B_3 \tilde{U} = \mu \tilde{U}, \tag{27}$$

which can be added to give

$$(A_3 + B_3) * \tilde{U} = (\lambda + \mu) * \tilde{U}. \tag{28}$$

Vector $\tilde{U}$ is therefore an eigenvector of matrix C_3. From the eigenvectors of matrices A_3 and B_3, the expression of the vector can be determined:

$$\tilde{U}_m(k) = \frac{1}{\sqrt{3}} \exp\left(\pm \frac{\mathrm{j}\pi(4m-3)(k-1)}{3} \right), \quad k, m = 1, 2, 3. \tag{29}$$

3.3. Simplifying vector $\tilde{U}$

Vector $\tilde{U}$ can be simplified to give real expressions which are also eigenvectors of matrix C_3. This simplification is given by the following formulas:

$$W_i = \frac{1}{\sqrt{2}} \{ \exp(\mathrm{j}\theta_i) * \tilde{U}_i + \exp(-\mathrm{j}\theta_i) * \tilde{U}_i^* \}. \tag{30}$$

$\tilde{U}_i^*$ is the complex conjugate of $\tilde{U}_i$. θ_i is an arbitrary angle. By varying θ_i, we obtain a whole discrete cosine transformation family (DCT), as for example, the transformation expression below:

$$W_m(k) = \begin{cases} \dfrac{1}{\sqrt{3}}, & m = 1, \quad k = 1, 2, 3, \\ \sqrt{\dfrac{2}{3}} \cos\left\{ \dfrac{(2k-1)(m-1)\pi}{6} \right\}, & m = 2, 3, \quad k = 1, 2, 3. \end{cases} \tag{31}$$

Likewise we obtain the discrete sine transformation expression using the combination below:

$$Y_i = \frac{1}{\sqrt{2}} \{ \exp(\mathrm{j}\theta_i) * \tilde{U}_i - \exp(-\mathrm{j}\theta_i) * \tilde{U}_i^* \}. \tag{32}$$

We thus obtain the discrete odd sine transformation expression (DEST):

$$Y_m(k) = \begin{cases} \sqrt{\dfrac{2}{3}} \sin\left\{ \dfrac{(2k-1)m\pi}{6} \right\}, & m = 1, 2, \quad k = 1, 2, 3, \\ \dfrac{1}{\sqrt{3}} \sin\{(2k-1)\dfrac{\pi}{2}\}, & m = 3, \quad k = 1, 2, 3. \end{cases} \tag{33}$$

4. Application to colour images

The task is to compare the results of the Karhunen–Loève transformation with those of DCT and DEST transformations from colour images initially encoded under the RGB system. We first analyse the homogeneity of the images to put ourselves in the ideal conditions of approximation of the Karhunen–Loève space.

4.1. Analysis of colour image stationarity

Take the following two images:

House

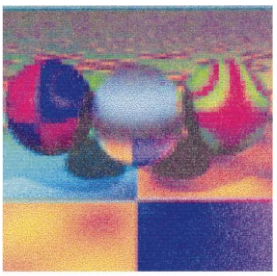

Baubles

The House image is a colour picture of a natural scene whereas the Baubles picture is computer generated. The correlation matrices calculated for the two images are

$$\varphi_{\mathrm{M}} = \begin{pmatrix} 1.00 & 0.87 & 0.80 \\ 0.87 & 1.00 & 0.89 \\ 0.80 & 0.89 & 1.00 \end{pmatrix}, \qquad \varphi_{\mathrm{B}} = \begin{pmatrix} 1.00 & 0.24 & -0.41 \\ 0.24 & 1.00 & -0.25 \\ -0.41 & -0.25 & 1.00 \end{pmatrix}.$$

House correlation matrix Bauble correlation matrix

By comparing the correlation matrices of the two images, we conclude that the House image, with a mean correlation coefficient of 0.91 is more homogeneous than the baubles image with a mean correlation coefficient of -0.42.

Consider the correlation matrix of a colour image in the RVB system below:

$$\varphi_I = \begin{pmatrix} 1 & \varphi_{12} & \varphi_{13} \\ \varphi_{12} & 1 & \varphi_{23} \\ \varphi_{13} & \varphi_{23} & 1 \end{pmatrix}. \tag{34}$$

The mean error committed by approximating this matrix to a first-order Markov process matrix is given by τ expressed below:

$$\tau = \frac{1}{3}\left[\frac{|\varphi_m - |\varphi_{12}||}{\varphi_m + |\varphi_{12}|} + \frac{|\varphi_m - |\varphi_{23}||}{\varphi_m + |\varphi_{23}|} + \frac{|\varphi_m^2 - |\varphi_{13}||}{\varphi_m^2 + |\varphi_{13}|}\right], \tag{35}$$

where

$$\varphi_m = \frac{|\varphi_{12}| + |\varphi_{23}|}{2}.$$

The coefficient of correlation calculated in the RVB space is linked to the coefficient of stationary that we have defined. The more φ tends to 1, the more τ tends to 0 and the image is stationary. If τ is high, that means

that the image is non-correlated in the origin basis. Consequently, the transformation of Karhunen–Loève is not adapted: the coefficient of stationary τ can then be used to predict the significance of a KL transformation or its approximation. We can thus determine the errors committed by approximating on the images under study. On the House image, the error is $\tau_{\mathrm{M}} = 1\%$ whereas that obtained for the Baubles image is $\tau_{\mathrm{B}} = 25.5\%$. From these calculations we deduce that the House image displays colours closer to one another than the Baubles image. Approximation of the Karhunen–Loève space is therefore better on the House image than on the Baubles image.

4.2. *Determining the colour components in Karhunen–Loève (KL), DCT and DEST spaces*

4.2.1. *Decomposition of the House image*

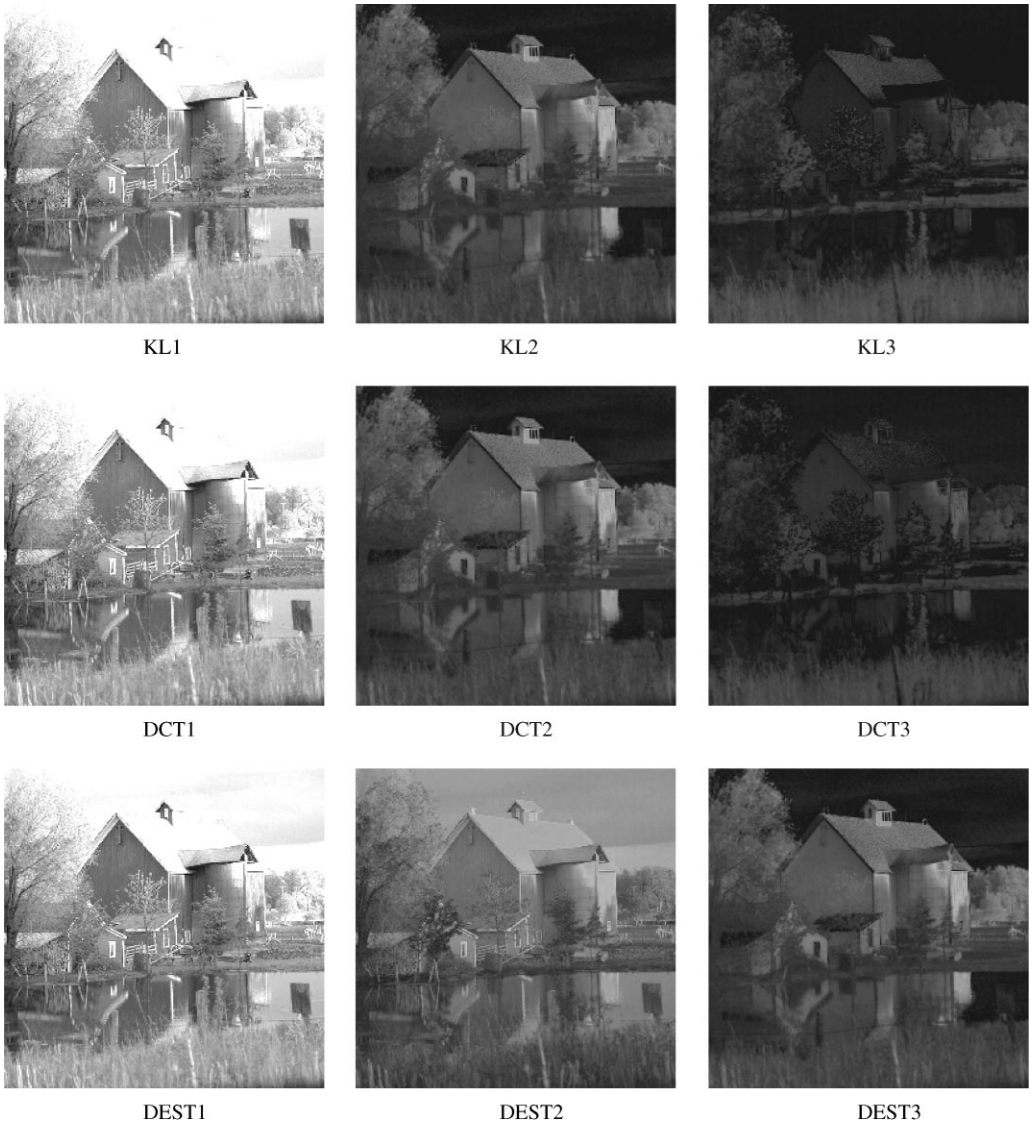

4.2.2. Decomposition of the Baubles image

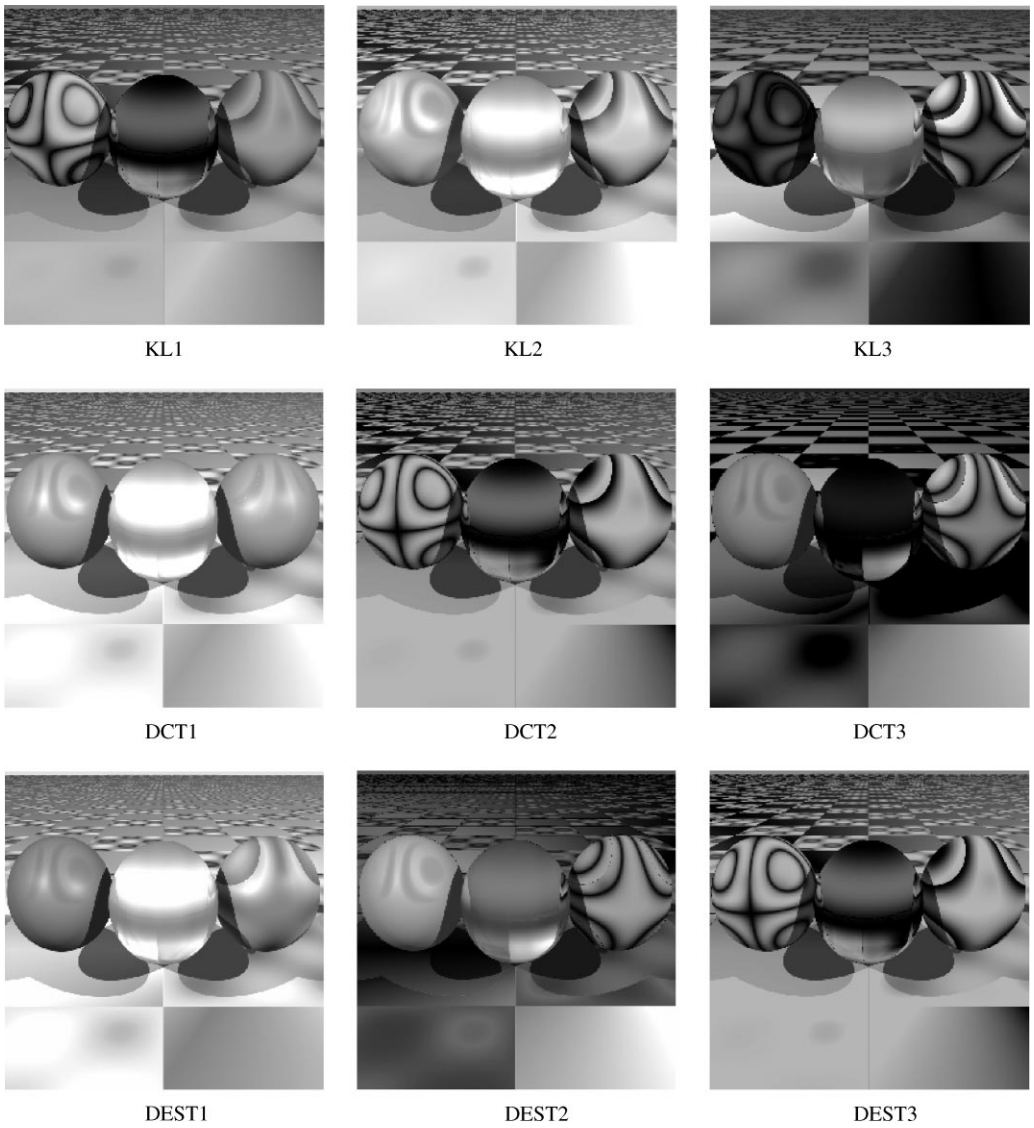

4.3. Analysis of results on approximated spaces

To characterise the DCT and DEST spaces obtained from approximation of the Karhunen–Loève space, we calculate the mean quadratic errors made on each approximated image. The Karhunen–Loève transformation, like the DCT and DEST transformations, provides three image planes representing the colour image. Each image is associated with a representation axis. The axes forming the Karhunen–Loève space are KL1, KL2 and KL3. The distribution of colour data is greater on KL1, average on KL2 and very low on KL3 when the image is homogeneously coloured. Otherwise, the colour information is uniformly distributed on the three axes. We also deduce axes DCT1 and DEST1 corresponding to KL1, DCT2 and DEST2 for

Table 1

House	DCT	DEST
Axis 1	0.047	6.670
Axis 2	0.00	0.00
Axis 3	0.021	6.183

Table 2

Baubles	DCT	DEST
Axis 1	27.04	25.53
Axis 2	7.50	7.50
Axis 3	4.83	12.17

Table 3
Mean quadratic errors E_q and homogeneity rate τ

Images	Plane	Pond	Woman	Lighthouse	Mountain	Parrots
E_q (DCT) (%)	0.187	0.09	1.13	0.30	0.037	0.21
τ (%)	4.54	0.2	9.5	3.87	0.23	0.54

KL2 and DCT3 DEST3 for KL3. The results of the comparisons expressed as percentages are summarised in Tables 1 and 2.

Analysis of Tables 1 and 2 shows that the approximation to Karhunen–Loève space by DCT and DEST spaces is better on the House image than on the Baubles one. These errors confirm the pervious results for the two images. As the House image is more stationary than the Baubles one, the approximation errors are lower.

We can also deduce from these tables that approximation of the Karhunen–Loève transformation by a DCT is more worth while than approximation by a DEST: the errors are smaller in DCT than DEST for both images.

We also analyse the approximation with other types of image. This was done to check experimentally the connection between the coefficient τ and the approximation errors. Table 3 gives, for each image, the coefficient of homogeneity τ and the mean quadratic errors obtained using a DCT approximation space.

By comparing these errors with coefficient τ, it can be deduced that the coefficient of homogeneity τ is indeed related to approximation errors: the lower the value of τ the lower the approximation error is. The homogeneity of a colour image can then be characterised by calculating coefficient τ. Experimentally, we determine a colour image as homogeneous for $\tau \leqslant 5\%$. But, for a video application (acquisition of images in real time), the stationary is preserved: two successive images are nearly similar. Consequently, it is not necessary to calculate the coefficient τ for each image. Thus, according to the film, the coefficient can be calculated for every 10–20 images or more to insure that the stationary condition remains in the tolerance defined.

5. Conclusion

By exploiting the properties of circular decomposition of Toeplitz matrices, we obtain interesting expressions for eigenvalues and eigenvectors of covariance matrices of stationary processes. From these

eigenvectors, it can be deduced that DCT, DEST, DFT transformation and all those derived from combinations of them approximate the Karhunen–Loève transformation.

Determining coefficient τ, as a measure of the homogeneity of a colour image, allows us a priori to characterise the approximation of the Karhunen–Loève space by the DCT or DEST space. For example, we found experimentally that for $\tau \leqslant 5\%$ colour images are homogeneous. Thus, in the case where colour images are homogeneous, representation of these images by the Karhunen–Loève space can be replaced by a representation in DCT or DEST space. This allows us to have a fixed and rapid transformation for all images to be analysed.

However, the approximation of Karhunen–Loève space by DCT space is more worth while than by DEST space. This study opens up significant perspectives for compressing colour images based on Karhunen–Loève space or approximations thereof.

References

[1] T. Carron, Segmentation d'images couleur dans la base Teinte–Luminance–Saturation: approche numérique et symbolique, Ph.D. Thesis, Univ. Savoie, France, 1995.
[2] M. Hamidi, J. Pearl, Comparison of the cosine and fourier transforms of markov-1 signals, IEEE Trans. Acoust. Speech Signal Process. (October 1976).
[3] R.K. Kouassi, J.C. Devaux, P. Gouton, M. Paindavoine, Application of the Karhunen–Loève transform for natural color images analysis, Irish Machine Vision and Image Process. Conf. 1 (1997) 20–27.
[4] J. Makhoul, On the eigenvectors of symmetric toeplitz matrices, IEEE Trans. Acoust. Speech Signal Process. ASSP-29 (4) (August 1981) 868–872.
[5] L. Ocadiz, Analyse en Composantes Principales d'une image couleur, Ph.D. Thesis, Univ. Grenoble, France, 1985.
[6] Y.I. Otha, T. Kanade, T. Sakai, Color information for region segmentation, Comput. Graphics Image Process. 13 (1980) 222–241.
[7] W.K. Pratt, Digital Image Processing, Mathematical Characterization of Continuous Images, Wiley, New York, 1978, pp. 1–90 (Chapter 1).
[8] W.K. Pratt, Digital Image Processing, Discrete two-Dimensional Linear Processing, Wiley, New York, 1978, Chapter 3, pp. 199–303.
[9] S. Shanmugam, Comments on discrete cosine transform, IEEE Trans. Comput. (July 1974).
[10] M. Unser, On the approximation of the discrete Karhunen–Loève transform for stationary processes, Signal Processing 7 (July 1984) 231–249.